

Author: Scott J. Menegon, Hing-Ho Tsang, John L. Wilson, Nelson T. K. Lam
Title: RC walls in Australia: displacement-based seismic design in accordance with AS 1170.4 and AS 3600
Year: 2021
Journal: Australian Journal of Structural Engineering
Volume: 22
Issue: 3
Pages: 205-221
URL: <http://hdl.handle.net/1959.3/461932>

Copyright: Copyright © 2021. Creative Commons Attribution 4.0 International (CC BY 4.0) license. This is the final Accepted Manuscript of an article published by Taylor & Francis in Australian Journal of Structural Engineering on 19 July 2021.

The published version is available at: <http://www.tandfonline.com/10.1080/13287982.2021.1954306>

RC walls in Australia: displacement-based seismic design in accordance with AS 1170.4 and AS 3600

Scott J. Menegon^{1,3*}, Hing-Ho Tsang^{1,4}, John L. Wilson¹ and Nelson T. K. Lam²

¹ Department of Civil and Construction Engineering, Swinburne University of Technology, Melbourne, Australia

² Department of Infrastructure Engineering, University of Melbourne, Melbourne, Australia

³ Scott J. Menegon ORCID: 0000-0001-6458-3637

⁴ Hing-Ho Tsang ORCID: 0000-0002-4912-5184

* Corresponding author, email: scott@menegon.com.au

Abstract: *Displacement-based methods, such as a non-linear static pushover analysis (e.g. the capacity spectrum method), have many advantages compared to traditional force-based design methods. However, implementing a non-linear analysis and design method in accordance with the Australian Standard for concrete structures (AS 3600) introduces many difficult technical issues into the design, of which the standard provides little guidance. The aim of this study is to provide a framework and general guidance for designers who wish to perform non-linear displacement-based analysis methods for RC wall buildings. The paper will present how these methods can be used in accordance with the Australian Standard for earthquake actions (AS 1170.4) to assess seismic compliance and then provide recommendations for the requirements stipulated by AS 3600, which includes an experimentally validated tension stiffening model, nonlinear stress-strain material curves, mean material properties and material strain limits. The paper is concluded with a case study example of how a displacement-based seismic assessment can be performed using a typical case study building.*

Keywords: Reinforced concrete (RC) walls; Tension stiffening; Nonlinear analysis; Displacement-based seismic design.

1 Trending towards displacement-based design

The seismic design and analysis of building structures have traditionally involved undertaking a force-based design procedure, where the structure is designed for a set of externally applied static forces that are meant to 'approximate' the effect of the earthquake ground shaking on the building. The forces are usually reduced by a force reduction factor (that varies based on the ductility of the structure) to indirectly account for inelastic behaviour that helps absorb the energy imposed from the earthquake ground shaking. Over the years, limitations and faults with force-based design procedures have been identified and many researchers began exploring new alternative 'displacement-based' design and assessment procedures. In the early 90's, Priestley (1993) authored a landmark paper titled *Myths and Fallacies in Earthquake Engineering – Conflicts Between Design and Reality* that summarised many of the problematic aspects of force-based seismic design; this included, for example, the broad assumption (or fallacy) that all structures of a similar basic structural form and level of detailing possess the same amount of ductility and general inelastic characteristics.

The general concept of displacement-based seismic design – as an alternative to force-based seismic design and its associated problematic aspects – has been around for some time in various forms. Displacement-based design could be defined quite broadly as any analysis or design procedure where displacement of the structure, as opposed to force or lateral strength, is primarily used to assess the seismic performance. Research studies were performed generally in the mid-70's by Shibata and

Sozen (1976) and mid-80's by Shimazaki and Sozen (1984). This was followed by research efforts in the late 80's by Priestley and Park (1987) with respect to reinforced concrete (RC) bridge structures and then more generally with respect to both RC frame buildings and RC wall buildings in the early 90's by Moehle (1992), Wallace and Moehle (1992) and Wallace (1994). In the mid-to-late 90's displacement-based assessment procedures were introduced into seismic evaluation and retrofit standards in the United States, ATC 40 (Applied Technology Council, 1996) and FEMA 273/274 (Federal Emergency Management Agency, 1997a; Federal Emergency Management Agency, 1997b).

In 2000, Priestley and Kowalsky (2000) published a journal paper titled *Direct Displacement-Based Seismic Design of Concrete Buildings*. The paper outlined the direct displacement-based design (DDBD) procedure and would later form part of the framework for the methodology presented in the text by Priestley, Calvi and Kowalsky (2007) titled *Displacement-Based Seismic Design of Structures*, which is considered the authority on the subject matter. In 2012, Sullivan, Priestley and Calvi (2012) released a proposed model code on the subject titled *A Model Code for the Displacement-Based Seismic Design of Structures*. The model code is primarily based on the recommendations made by Priestley et al. (2007). The DDBD procedure allows for structures to be designed to “achieve, rather than bounded by, a given performance limit state under a given seismic intensity”.

Despite nearly two decades passing since Priestley first publishing the DDBD procedure for buildings, the seismic design methodology for new buildings in earthquake design codes in many countries around the world, including Australia, remain largely focused towards force-based procedures. In the Australian context, previous studies have discussed displacement-based approaches in general terms, e.g. Wilson and Lam (2006), or proposed empirical backbone force-displacement models for individual RC elements, e.g. Wilson et al. (2015), Raza, Tsang and Wilson (2018) or Raza et al. (2019).

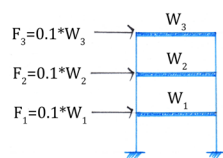
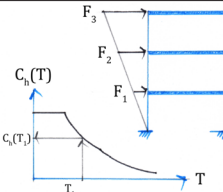
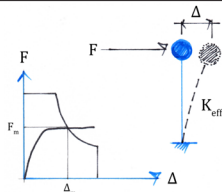
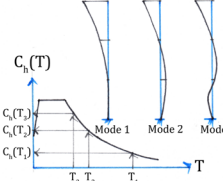
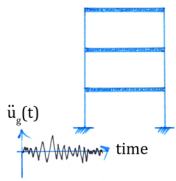
This paper is the third in a series of publications by the authors on the design of RC wall buildings in Australia. This series of publications are written with a distinct focus towards ‘design engineers’ and are intended to promote and educate the advanced design of RC walls and building cores with practitioners, while also presenting original research contributions to the literature.

The first paper in this series presented a reconnaissance survey and overview of multi-storey RC construction in Australia, which provided a snapshot of typical RC construction methods and detailing commonly used in the country (Menegon et al., 2017b). The second paper presented an overview of the seismic design methodology in Australia and the implications of relying on inelastic behaviour to resist the earthquake actions, i.e. trading strength for ductility. The paper then presented a critical review of widely observed detailing practices across the country that seemingly contradict the explicit design assumptions of force-based seismic design and the assumptions around ductility. The paper concluded with design recommendations and RC detailing advice for designers undertaking force-based seismic design (Menegon et al., 2018). This third paper presents a methodology for undertaking a displacement-based seismic design of an RC wall building in accordance with the Australian Standard for earthquake actions, AS 1170.4 (Standards Australia, 2007) and the Australian Standard for concrete structures, AS 3600 (Standards Australia, 2018). The paper makes recommendations for the various requirements stipulated by AS 3600 for undertaking a non-linear assessment, which include the adoption of an appropriate tension stiffening model, non-linear stress-strain material curves, mean material properties and material strain limits. The paper is concluded with a case study example, which illustrates how the method is implemented in practice.

2 Displacement-based design to Australian Standards

2.1 AS 1170.4 analysis procedures

The Australian Standard for earthquake actions, AS 1170.4 requires different levels of analysis depending on the earthquake design category (EDC) of the building. The EDC is a function of the Importance Level of the building, the seismic design hazard, the sub-soil class of the site and the overall height of the building. EDC I requires a static analysis where the lateral force at each storey is equal to 10% of the seismic weight of that respective storey; EDC II requires an equivalent static analysis where the lateral force is determined based on the fundamental natural period of the building and the response spectrum from the standard; while with EDC III, dynamic analysis is required. The procedures for EDC I, II and III are outlined in Sections 5, 6 and 7 of AS 1170.4, respectively. Most designers perform either an equivalent static analysis (i.e. Section 6) or multi-modal dynamic analysis (i.e. Section 7); both of which are force-based analysis methods. The analysis methods allowed by AS 1170.4 are summarised in Figure 1.

	Linear analysis*	Non-linear analysis†
EDC I static analysis AS 1170.4 Section 5	 <p>nominal lateral loads</p>	NA
EDC II static analysis AS 1170.4 Section 6	 <p>equivalent static analysis</p>	 <p>capacity spectrum method</p>
EDC III dynamic analysis AS 1170.4 Section 7	 <p>multi-modal dynamic analysis</p>	 <p>non-linear time history analysis</p>

* Linear analysis methods in AS 1170.4 indirectly account for inelastic behaviour using a force reduction factor equal to μ/S_p .

† Non-linear analysis methods in AS 1170.4 directly account for inelastic behaviour through the adoption of non-linear material models in the analysis.

Figure 1: AS 1170.4 analysis methods matrix.

In a subtle move towards displacement-based seismic design and assessment methodologies, the 2007 version of AS 1170.4 introduced Clause 6.5, which says “it shall be permissible to determine μ [ductility factor] and S_p [structural performance factor] by using a non-linear static pushover analysis”. The AS 1170.4 commentary (Wilson and Lam, 2007) further elaborates on this statement by saying that in this instance, the capacity spectrum method (CSM) can be adopted in lieu of using an equivalent static analysis method for EDC II. The adoption of the CSM is only appropriate for low- to

mid-rise buildings that are first-mode dominant; thus, the assessment can be conducted based on an equivalent single-degree-of-freedom (SDOF) model.

The CSM is a pushover analysis wherein the earthquake performance of a structure is assessed by overlaying the structure's capacity curve (i.e. its force-displacement pushover response) on an acceleration-displacement response spectrum (ADRS), which is a visual representation of the earthquake demand on a building. Both the capacity and demand curves are obtained via an idealised SDOF system that represents the building structure.

An ADRS curve is constructed by plotting the response spectral acceleration values (i.e. RSa) against the response spectral displacement values (i.e. RSd). The RSa can be calculated based on Equation 6.2(5) in AS 1170.4 (which is shown in Figure 2(a)). The Z value is defined in AS 1170.4 as the location-specific hazard design factor that is the equivalent of the design peak ground acceleration (PGA) (in the unit of gravitational acceleration, i.e. g), such that a design force can be obtained when Z is multiplied by the seismic weight of the structure W_t (see Section 6.2.1 of AS 1170.4 for details). Hence, assigning a unit of g back to the value obtained from Equations 6.2(5) gives RSa in the unit of g . The other variables k_p and $C_h(T)$ are the probability factor and spectral shape factor, respectively. The former adjusts Z for different return period events and the later defines the overall shape of the response spectrum. An example design response spectrum is plotted in Figure 2(a) for a typical site with a $k_p Z$ value of $0.08g$.

The corresponding response spectral velocity and displacement values (i.e. RSv and RSd , respectively) can be calculated based on Equations 1 and 2. When converting the RSa to RSv or RSd , care should be taken in considering the units, since RSa is typically expressed with the units of g , whereas the RSv and RSd are typically expressed in terms of mm/s and mm , respectively. The velocity and displacement response spectra for a $k_p Z$ value of $0.08g$ are shown in Figures 2(b) and 2(c), respectively. These figures also show the various spectra for rock (B_e), soil (C_e), deep/soft soil (D_e) and extremely soft soil (E_e) sites. The site classes in AS 1170.4 are descriptive classifications based on soil depth and generic soil descriptions and/or properties. For addition information, a refined site classification scheme based solely on site natural period and the corresponding set of response spectra with a displacement focus have recently been proposed by Tsang, Wilson and Lam (2017b), based upon a theoretical framework they developed that takes into account the effects of soil resonance (Tsang, Chandler and Lam, 2006; Tsang et al., 2017a). Site classification based on site natural period has become a major trend in recent developments of seismic design codes (e.g. Looi, Tsang and Lam, 2019; Pitilakis et al., 2019).

$$RSv = RSa \times \left(\frac{T}{2\pi}\right) \quad \dots 1$$

$$RSd = RSv \times \left(\frac{T}{2\pi}\right) = RSa \times \left(\frac{T}{2\pi}\right)^2 \quad \dots 2$$

AS 1170.4 requires that the ADRS diagram (both acceleration and displacement demand) be increased by a factor of 1.5 when undertaking displacement-based assessment methods, as shown in Figure 2(d). This 1.5 factor is required since the direct nature of using a displacement-based procedure results in some of the uncertainties associated with seismic design not being accounted for, which are otherwise absorbed due to the less direct and conservative aspects of force-based design. These uncertainties are associated with both the challenges of predicting the seismic hazard and displacement demand due to the limited database of historical events available in low to moderate intraplate seismic regions (as compared to interplate regions of higher seismicity), and the challenges of predicting the displacement capacity of inelastic structural systems.

The ADRS diagram, as shown in Figure 2(d), has the units of g's and mm's. The vertical axis of the ADRS can be converted to force by multiplying it by the effective seismic weight (which has the units kN's) of the respective structure under consideration. Once the ADRS has been converted to have the units of force on the vertical axis and displacement on the horizontal axis, the non-linear capacity curve of the structure can be overlaid to determine the seismic performance. This procedure is illustrated further at the end of the paper using a case study example.

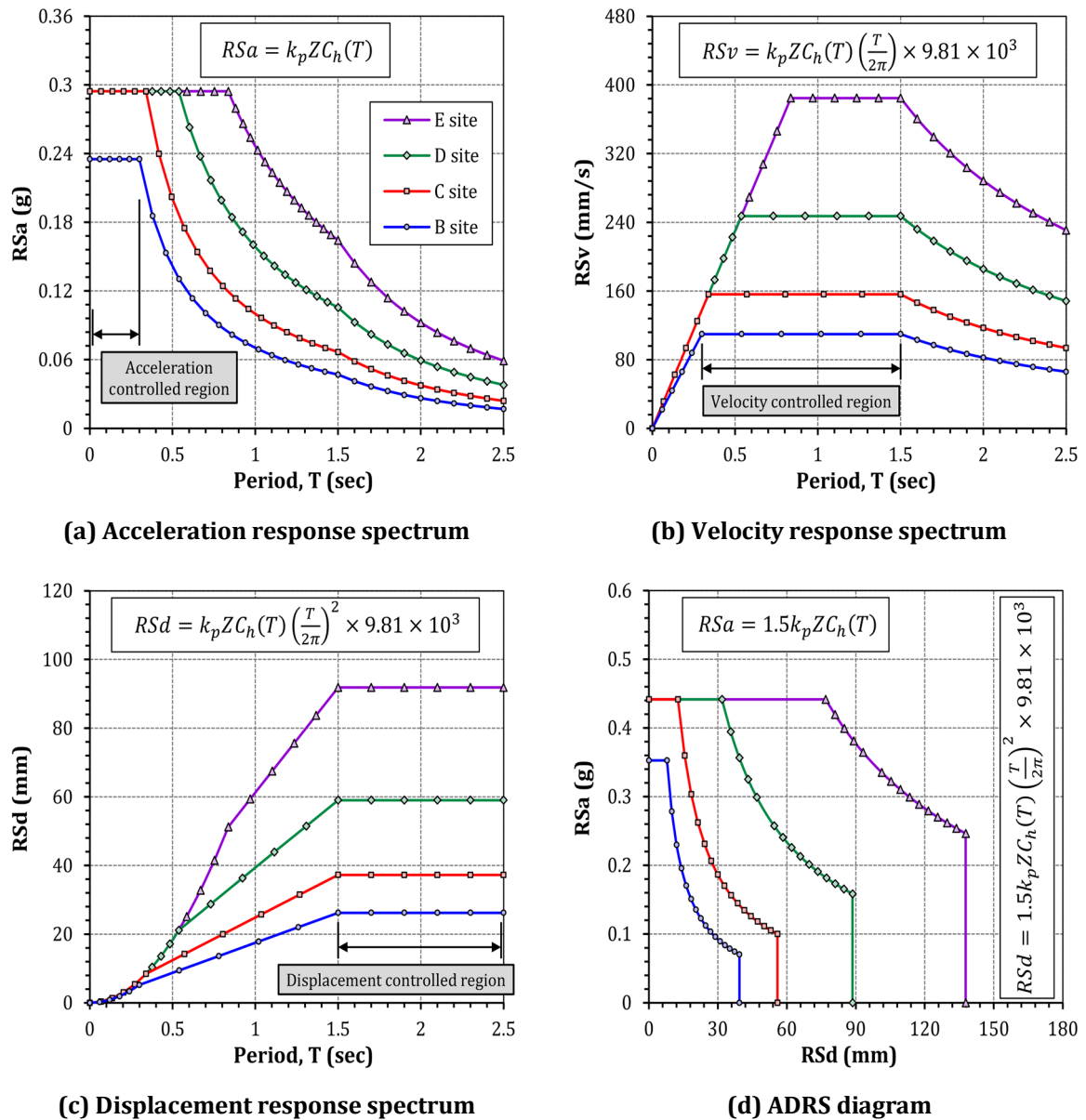


Figure 2: AS 1170.4 response spectrum for a seismic design hazard ($k_p Z$) of 0.08g.

2.2 AS 3600 non-linear design methods

Implementing the CSM approach for an RC building in a design office scenario introduces many difficult technical issues if one wants to comply with the Australian Standard for concrete structures, AS 3600, when calculating the non-linear capacity curve of the structure. The Standard has a number of requirements for non-linear analysis methods, of which little guidance is provided in either the standard itself or the commentary. These requirements include the adoption of an appropriate tension

stiffening model, nonlinear stress-strain material curves, mean material properties and material strain limits. Each of these items are addressed in subsequent sections of this paper in the context of the non-linear performance of an RC wall building, which utilises RC walls and RC building cores as the primary lateral load resisting elements. AS 3600 also requires a sensitivity analysis to be performed to assess how sensitive the results of the analysis are to variations in the input data and modelling parameters. A sensitivity analysis is performed as part of the case study example at the end of the paper. The results of this analysis and key observations are discussed accordingly.

3 Tension stiffening in RC walls

Reinforced concrete walls subjected to in-plane lateral loads develop axial compressive and tensile forces at each end of the wall, respectively, to resist the overturning moments generated from the applied in-plane loading. The tensile forces are initially resisted in combination by both the concrete and vertical reinforcement until the maximum tensile stress of the concrete has been exceeded and cracking occurs. At each crack location, the tensile resistance is solely provided by the vertical reinforcement. However, between adjacent cracks, the mechanical interlock between the reinforcement and concrete (i.e. bond) allows a portion of the tensile force to be distributed back into the concrete between adjacent cracks. This behaviour ‘stiffens’ up the cracked tensile region of the wall and is called tension stiffening.

The tension stiffening behaviour means the localised reinforcement strains at each crack location are different to the average tensile strains in the concrete cross-section, as illustrated in Figure 3. Menegon et al. (2021b) proposed a simple tension stiffening model for converting local reinforcement tensile strains (that would otherwise usually be used for ‘balancing the stress block’ while calculating a non-linear moment-curvature response of the section) to average global strains in the concrete cross-section, which would provide modified curvature values that account for tension stiffening of the cross-section. This process is broadly illustrated in Figure 3.

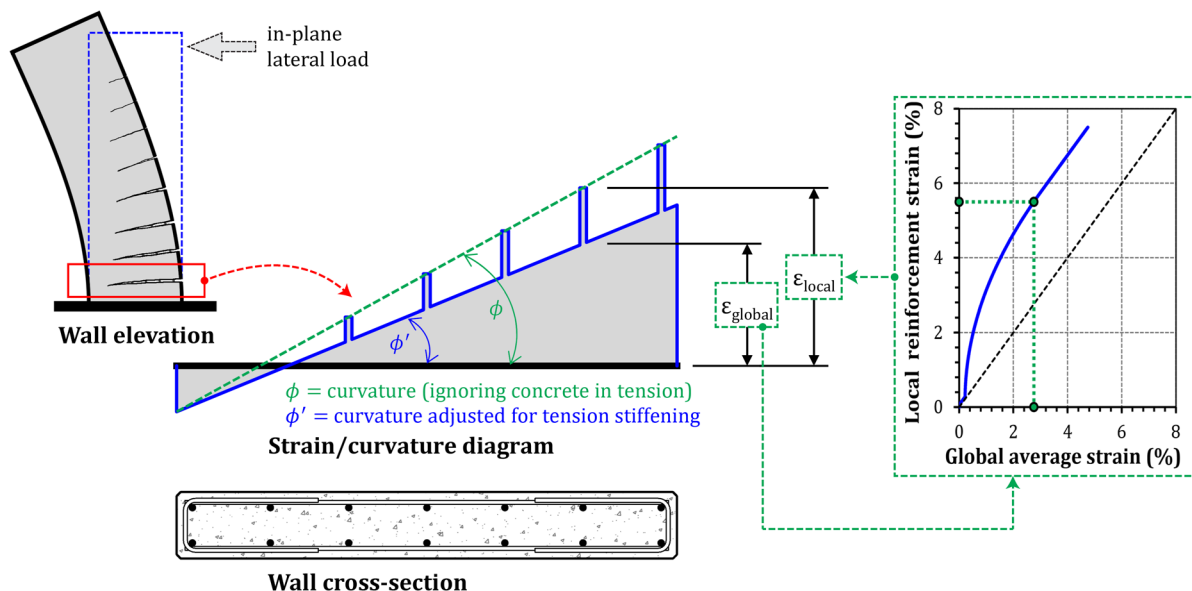


Figure 3: Tension stiffening in RC walls subject to in-plane loading.

The simplified Menegon et al. (2021b) tension stiffening model is determined using Equations 3 to 6, where ϵ_G is the global average strain, determined using ϵ_s the local reinforcement strain. An example of the relationship determined using the proposed model is also shown in Figure 3. The model is

primarily dependent on the: stress-strain properties of the reinforcement; ultimate tensile stress of the concrete (f_t); vertical reinforcement ratio ($p_v = A_{sv}/A_g$, where A_{sv} is the area of vertical reinforcement and A_g is the gross cross-sectional area of the wall); and a factor α_1 , which is dependent on the bar size and equals 0.36, 0.40, 0.42, 0.44 and 0.45 for 12, 16, 20, 24 and 28 mm diameter bars, respectively. The model is based on a simple bilinear stress-strain relationship, which is defined by the yield stress (f_{sy}), yield strain (ε_{sy}), ultimate stress (f_{su}) and ultimate strain (ε_{su}) of the reinforcement. An example of the bilinear stress-strain model is presented in the following section. The case study example provided at the end the paper implements this tension stiffening model.

Elastic reinforcement strains, $\varepsilon_s < \varepsilon_{sy}$:

$$\frac{2\varepsilon_s E_s}{k_2} \leq 1: \quad \varepsilon_G = \frac{\varepsilon_s^2 E_s}{k_2} \quad \dots 3$$

$$\frac{2\varepsilon_s E_s}{k_2} > 1: \quad \varepsilon_G = \varepsilon_s - \frac{0.25k_2}{E_s} \quad \dots 4$$

Inelastic reinforcement strains, $\varepsilon_s > \varepsilon_{sy}$:

$$\frac{2(\varepsilon_s - \varepsilon_{sy})k_3}{k_2} \leq 1: \quad \varepsilon_G = \varepsilon_{sy} - \frac{0.25k_2}{E_s} + \frac{k_3}{E_s k_2} [\varepsilon_s - \varepsilon_{sy}] [k_2 + (\varepsilon_s - \varepsilon_{sy})(E_s - k_3)] \quad \dots 5$$

$$\frac{2(\varepsilon_s - \varepsilon_{sy})k_3}{k_2} > 1: \quad \varepsilon_G = \varepsilon_s - \frac{0.25k_2}{k_3} \quad \dots 6$$

Where:

$$k_2 = 1.2f_t \left(\frac{1}{p_v} - 1 \right) \quad \text{and} \quad k_3 = \frac{\alpha_1 E'_s}{0.15} \quad \dots 7$$

4 Stress-strain material models

4.1 Concrete

Considerable research efforts have been devoted over the last 50 years to developing reliable stress-strain material models for concrete. This included several studies at the University of Canterbury in the 70's and 80's to develop models for both confined and unconfined concrete. This initially resulted in the *Kent and Park model* in 1971 (Kent and Park, 1971), which was later followed by the *Modified Kent and Park model* in 1982 (Park, Priestley and Gill, 1982; Scott, Park and Priestley, 1982). The initial Kent and Park model only allowed for an increase in strain due to the confinement steel and made no allowance for an associated increase in compressive stress. Whereas the modified version allowed for an increase in the maximum compressive stress based on the confinement steel.

The Modified Kent and Park model was then followed by the Mander, Priestley and Park (1988) model for confined and unconfined concrete. The Mander et al. (1988) model is a widely used and one of the most highly cited stress-strain material models for concrete. The model was recently used in a theoretical study by the authors to predict the backbone non-linear force-displacement behaviour of 16 RC wall specimens. Very good correlation with the test data was observed in this study (Menegon et al., 2020a). The Mander et al. (1988) model was however only developed and validated against test specimens constructed using normal strength concrete. Therefore it is being recommended for modelling walls that are constructed using normal strength concrete (i.e. $f'_c \leq 50$ MPa).

For situations where high strength concrete (i.e. $f'_c > 50$ MPa) is being specified, the more recent Karthik and Mander (2011) model for confined and unconfined concrete is being proposed. The unconfined model was largely based on the unconfined model proposed previously by Collins, Mitchell and MacGregor (1993), which is widely cited as an appropriate model for high strength unconfined concrete. The confined model was developed using the experimental results from Li, Park and Tanaka (2000), which included specimens with concrete compressive strengths up to 83 MPa. The confined and unconfined Mander et al. (1988) and Karthik and Mander (2011) models are presented in Figures 4(a) and 4(b), respectively. The reader is directed to each of these respective references for the implementation of these models. Guidance regarding the implementation of the Mander et al. (1988) model can also be found in Priestley, Seible and Calvi (1996) or Priestley et al. (2007).

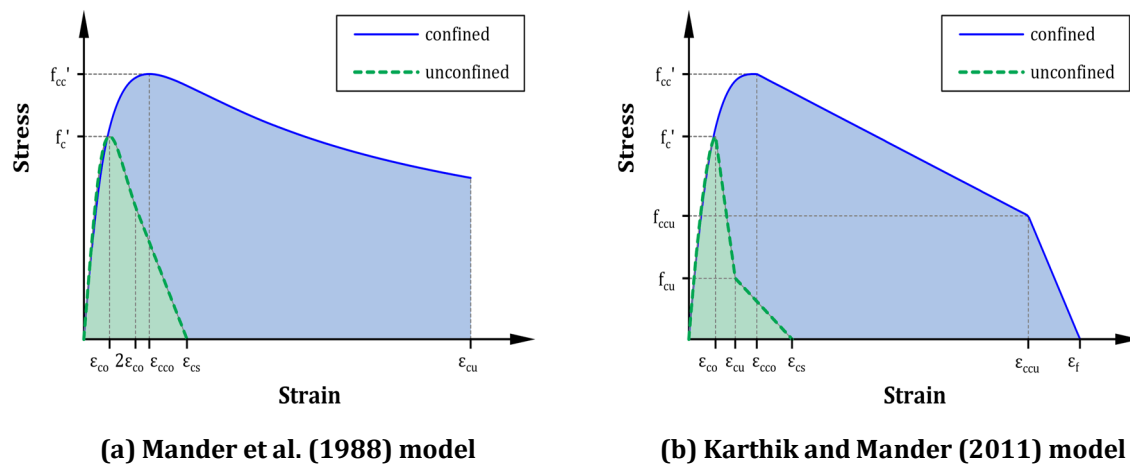


Figure 4: Stress-strain material models for (a) normal strength concrete ($f'_c \leq 50$ MPa) and (b) high strength concrete ($f'_c > 50$ MPa).

4.2 Reinforcement

The stress-strain behaviour of reinforcement is largely dependent on whether the reinforcement is supplied in straight lengths or coils. The former generally has a very distinct yield plateau region before the onset of strain hardening occurs under monotonic loading. Whereas the latter generally has no distinguishable yield plateau region and the transition from elastic response to inelastic strain hardening occurs over a larger region of strain, as opposed to a very sharp elastic to inelastic transition point. This varying stress-strain behaviour is shown in Figure 5(a). Generally, 10 mm nominal diameter reinforcing bars are supplied in coils, 12 mm nominal diameter reinforcing bars are supplied in either coils or straight bars and 16 mm nominal diameter and greater reinforcing bars are typically supplied as straight lengths.

The yield stress of bars supplied in straight lengths is quite obvious upon inspecting a typical stress-strain response curve (taken from a simple monotonic test). Bars supplied in coils however, that typically have no clearly identified yield point, the yield stress is taken as the 0.2% proof stress (Standards Australia and Standards New Zealand, 2019). The 0.2% proof stress is taken as the stress corresponding to the intersection of the actual stress-strain response curve and a line drawn from 0.2% strain at a slope of E_s (i.e. the elastic modulus of the bar).

A simple bilinear strain-strain model is being proposed for modelling reinforcement. The bilinear model consists of two stages. The first stage is the elastic response stage that consists of a straight line from the origin with a slope of E_s (i.e. the elastic modulus of the reinforcement) up until the yield stress (i.e. f_{sy}) and corresponding yield strain (i.e. ϵ_{sy}) of the bar is reached. The second stage is the inelastic

response stage that consists of a second straight line from the yield point to the point corresponding to the ultimate strain (i.e. uniform elongation or ϵ_{su}) and ultimate stress (i.e. f_{su}). The slope of this line is equal to the inelastic modulus (i.e. E'_s). The bilinear model is illustrated in Figure 5(b).

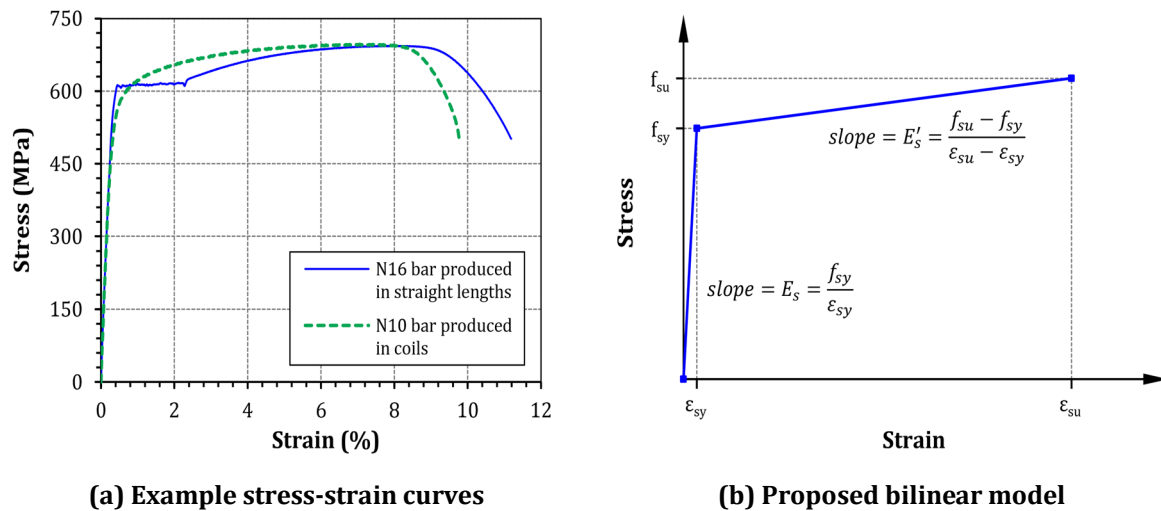


Figure 5: Stress-strain behaviour of reinforcement.

5 Mean material properties

One of the more challenging aspects of undertaking non-linear analysis in accordance with AS 3600 is the selection of appropriate values for the mean material properties. AS 3600 stipulates that all non-linear analysis methods to use “mean values of all relevant material properties” and the current commentary, AS 3600–2009 Supp 1 (Standards Australia, 2014), further states that for “non-linear and other refined methods of analysis, actual stress-strain curves, using mean rather than characteristic values, should be used”.

Recommendations for expected mean material strengths for standard grades of concrete and reinforcement used in Australia will be presented in the following two sub-sections based on a comprehensive database of material test data assembled by the authors, which included 3,447 cylinder test results and 15,201 reinforcement tensile test results taken over the period from 2009 to 2020, and is presented in a separate paper (Menegon et al., 2021a).

5.1 Mean strength of concrete

Concrete is usually specified for a given characteristic 28-day compressive strength (i.e. f'_c). Concrete in Australia is normally specified as a ‘normal’ grade, which for slabs on ground would typically be N25, suspended slabs N32 and structural walls and columns in low-rise buildings either N40 or N50. However, this does vary greatly with the discretion of the designer and the individual circumstances. These grades have characteristic 28-day compressive strengths of 25, 32, 40 and 50 MPa, respectively. Alternatively, ‘special’ grades can be specified, which are usually high-strength grades and generally consist of S65, S80 and S100. These grades have characteristic 28-day compressive strengths of 65, 80 and 100 MPa, respectively. However, special grades can also be specified when other performance requirements are needed, such as early age strength.

For non-linear analysis methods the mean in-situ strength of concrete (i.e. f_{cmi}) should be used with the non-linear stress-strain material curve presented in the previous section. The characteristic strength can be converted to an in-situ mean strength using Equation 8, where K_1 accounts for the

difference between the characteristic 28-day cylinder strength and the mean 28-day cylinder strength, i.e. $K_1 = f_{cm}/f'_c$; K_2 accounts for the difference between the mean cylinder strength and the actual in-situ strength, i.e. $K_2 = f_{cmi}/f_{cm}$, which varies due to the different curing conditions between the in-situ structure and the cylinder samples; and K_3 accounts for the difference between the 28-day strength of the concrete and the long-term strength of the concrete (i.e. the strength gain with time).

$$f_{cmi} = K_1 K_2 K_3 f'_c \quad \dots 8$$

While there was some level of uncertainty and variation observed in Menegon et al. (2021a) for the K_1 ratio, which is not surprising given the inherent variability involved with concrete production, it was broadly found that the mean cylinder strength of concrete was 1.2 times the characteristic strength for concrete grades N20 to S65 and 1.1 times for S80 and S100. Further, the K_2 factor was recommended to be taken as 0.88 and finally, it was recommended to ignore any long-term strength development (i.e. $K_3 = 1.0$) based on observations from studies presented in Neville (1996), wherein it was noted that “in the absence of definite moist curing, no increase in strength should be expected with age” for in-situ concrete. Therefore, the mean in-situ strength of concrete for non-linear analysis is being recommended to be taken as 1.06 times the characteristic strength for concrete grades N20 to S65 and 0.97 times the characteristic strength for concrete grades S80 and S100, as shown in Equations 9 and 10, respectively.

Concrete grades N20 to S65:

$$f_{cmi} = 1.06 f'_c \quad \dots 9$$

Concrete grades S80 and S100:

$$f_{cmi} = 0.97 f'_c \quad \dots 10$$

5.2 Mean strength of reinforcement

AS 3600 (Standards Australia, 2018), requires reinforcement to be produced and manufactured in accordance with AS/NZS 4671 (Standards Australia and Standards New Zealand, 2019), which allows reinforcement to be produced as one of three ductility grades: ‘L’ grade, i.e. low-ductility class; ‘N’ grade, i.e. normal-ductility class; or ‘E’ grade, i.e. earthquake-ductility class. L and N grades are primarily produced for Australia and E grade is primarily produced for New Zealand. E grade reinforcement is typically quite difficult to source in Australia and as such, rarely specified in building or infrastructure projects. The most common grade of reinforcement used for detailing RC walls in Australia is grade D500N, which denotes deformed N grade bars with a characteristic yield stress of 500 MPa. While mean material data is presented for D500L, D500N, D300E, D500E, R250N and R500N reinforcement in Menegon et al. (2021a), recommendations in this paper will be for D500N only, since it is the primary type of reinforcement used in lateral load resisting elements in Australia. While D500L is occasionally specified in precast concrete wall panels, it is not recommended due to its low ductility (refer Menegon et al. (2018) for a detailed discussion).

Based on the trends in mean properties, which were varied based on supplier, three scenarios of mean material properties for D500N reinforcement are being recommended for the use in non-linear analysis as summarised in Table 1. The first scenario is based on the overall mean values of the complete D500N dataset, while the second and third scenarios are supplier specific scenarios that are based on the two distinct manufacturing targets observed from different suppliers. The intent is that the non-linear analysis procedure used by the designer would be repeated for each of these different scenarios of mean material properties.

Table 1: Proposed scenarios of mean material properties for D500N reinforcement.

Scenario	f_{sy} (MPa)	f_{su} (MPa)	f_{su}/f_{sy}	ϵ_{su} (%)	E_s (MPa)	E'_s (MPa)
1 (overall mean)	550	670	1.22	10.3	190,000	1,199
2 (supplier scenario 1)	530	690	1.29	12.0	190,000	2,531
3 (supplier scenario 2)	560	635	1.13	6.6	190,000	641

6 Material strain limits and performance criteria

When undertaking a pushover analysis, material strain limits are required to govern/dictate when ultimate failure occurs (i.e. the ultimate limit state capacity of the structure is achieved), in addition to other pertinent performance points. Strain limits are proposed for the ‘effective stiffness’ point, which is used for assigning an effective (cracked) stiffness to an RC element; the ‘yield moment’ point, which is the transition point from elastic to inelastic response when a simplified bilinear response is taken (as discussed in the following case study section); and the ‘ultimate’ point, which is the point corresponding to the ultimate limit state capacity (ULS) being achieved. The proposed strain values are summarised in Table 2, with a subsequent discussion for the rationale behind each value.

Table 2: Proposed material strain limits.

Performance point	Concrete compression strain limit, ϵ_c	Reinforcement tension strain limit, ϵ_s
Effective stiffness	0.002	ϵ_{sy}
Yield moment	0.003	0.015
Ultimate (ULS)	0.006	0.040

The proposed material strain limits apply to limited ductile RC walls with an associated level of detailing outlined in AS 3600. Limited ductile construction is the most common form of construction (in terms of ductility classification) in Australia. Limited ductile RC walls typically have minimal or no confinement (i.e. ligatures) and are detailed with a constant spaced grid of horizontal and vertical bars on each face of the wall with ‘U’ bars at the ends of the walls, which are lapped with the horizontal reinforcement.

The reader should note that the material strain limits proposed in Table 2 are slightly different to the values proposed previously by the authors in Menegon et al. (2019b). The ULS tensile strain limit has been decreased from 0.05 to 0.04 following the subsequent publication and findings of experimental tests results (Menegon et al., 2019a), as further discussed below. The yield moment criteria are also different since in this instance it is being used to primarily create a simplified bilinear response that appropriately and reasonably matches the *actual* response for design purposes. Whereas, the “true yield strength” (corresponding to a damage state of Moderate Damage) in Menegon et al. (2019b) is used for defining an *actual* damage state that can be used as part of the framework proposed therein for undertaking seismic vulnerability and risk assessments.

6.1 Effective stiffness criteria

The effective stiffness is being proposed to be taken as when either the yield stress (ϵ_{sy}) is reached in the extreme tensile face reinforcing bar or a compressive strain of 0.002 is reached in the extreme compressive fibre of the section, whichever occurs first. A compressive strain of 0.002 corresponds to the “yield strain” of concrete in the Mander et al. (1988) model discussed previously.

6.2 Yield moment criteria

The yield point is being proposed to be taken as when either a tension strain of 0.015 is reached in the extreme tensile face reinforcing bar or when a compressive strain of 0.003 is reached in the extreme compressive fibre of the section, whichever occurs first. The 0.015 tensile strain limit corresponds to the recommendation in Priestley et al. (2007) for a serviceability limit state and is based on ensuring a residual crack width of 1.0 mm or less is maintained. Priestley et al. (2007) also recommends a serviceability compressive strain limit of 0.004 for concrete, based on it being a conservative lower limit for the initiation of spalling, however a more conservative value of 0.003 is being proposed herein since limited ductile walls usually have minimal or no confinement in the end regions of the wall compared to ductile walls commonly seen in higher seismic regions like New Zealand or the west coast of the United States.

6.3 Ultimate criteria

AS 3600 does not specify material strain limits for a non-linear pushover analysis. The code does specify a compression strain limit of 0.003 in the compression reinforcement, however this requirement is specified in the context of determining the strength of an RC column (i.e. interaction-diagram). No limits are specified for tensile strains in reinforcement.

The 0.006 compression strain limit proposal is based on the recommendations from Sullivan et al. (2012) for the ‘no collapse’ performance objective, which is broadly the same performance objective in AS/NZS 1170.0 Standards Australia and Standards New Zealand (2002) since it defines ultimate limit state as the “states associated with collapse, or with similar forms of structural failure”. This proposed limit is based on assuming no confinement in the end regions of the walls, which is typical for limited ductile walls. However, if there’s an instance where no lapped ‘U’ bars are provided at the ends of walls, then this limit should likely be further reduced to 0.004. Similarly, if confinement is provided in the end regions of walls, then the 0.006 compression strain limit could be increased by using Equation 11 proposed in Sullivan et al. (2012), which is originally presented in Priestley et al. (2007). The reader is directed to either of these references for further implementation of this equation.

$$\epsilon_{cu} = 1.5 \times \left[0.004 + \frac{1.4\rho_v f_{sy.f} \epsilon_{su.f}}{f_{ccmi}} \right] \leq 0.03 \quad \dots 11$$

Where: ρ_v is the volumetric ratio of confinement reinforcement; $f_{sy.f}$ is the yield stress of the confinement reinforcement; $\epsilon_{su.f}$ is the ultimate strain of the confinement reinforcement; and f_{ccmi} is the confined concrete in-situ mean strength.

The 0.04 tension strain limit proposal is to ensure local bar buckling of the vertical reinforcement does not occur under reversed cyclic loading. It was shown experimentally in Menegon et al. (2019a) that an RC element could sustain local tension strains in the vertical reinforcement of about 0.06–0.07 before being susceptible to bar buckling on reversed load cycles. This is however a very complex failure mechanism and due to other experimental testing where lower tensile strains of 0.042–0.056 (approximately) were observed prior to local bar buckling occurring, Menegon et al. (2019a)

recommended a lower bound maximum tensile strain limit of 0.04. Similar to the point above, if tightly spaced confinement is provided in the end regions of walls that restrains the vertical bars, then an increased tension strain limit could be adopted. In this instance, the Priestley et al. (2007) and Sullivan et al. (2012) recommendation of $0.9\varepsilon_{su}$ (with an upper limit of 0.08) is proposed, however they stipulate to achieve this level of tension strain without bar buckling occurring, bar restraints (i.e. confinement) are required at a maximum spacing of $s = [3 + 6(f_{su}/f_{sy} - 1)]d_b$, where d_b is the bar diameter of the vertical reinforcement.

6.4 Other performance considerations

The limits proposed above do not provide any consideration for avoiding other commonly seen failure mechanisms in walls, such as out-of-plane buckling instabilities that have been observed in both post-earthquake reconnaissance (Elwood, 2013) and laboratory testing programs (Dashti, Dhakal and Pampanin, 2017; Menegon et al., 2019a). The current 2018 version of AS 3600 introduced slenderness ratios (i.e. inter-storey height to thickness ratios), which are meant to apply to any plastic hinge region of a wall, of 20 and 16 for limited ductile ($\mu = 2$) and moderately ductile ($\mu = 3$) walls, respectively. These ratios could be adopted based on the broad amount of ductility observed in the pushover analysis for the structure. Alternatively, the model proposed by Chai and Elayer (1999) could also be used to calculate maximum tension strains (on a case-by-case basis) to prevent failure mechanisms of this nature.

Further, the 1.5% maximum drift provision of AS 1170.4 needs to be complied with in the design of the building and thereby limiting the displacement demand. This 1.5% drift limit needs to be checked for the worst scenario, which is typically at the corners of the floor plan due to torsional effects from plan asymmetry of mass or lateral stiffness, and not just at the centre of mass where the load is applied.

7 Case study

This section presents the implementation of the capacity spectrum method (CSM) using the methodology presented in this paper for a typical case study building.

7.1 Case study building

The case study building adopted for this example is shown in Figure 6 and is denoted CSB7a. The designation CSB7a is with reference to a series of other case study buildings developed by the authors and presented in Menegon et al. (2019b), which have been used for seismic vulnerability studies of RC buildings in Australia.

CSB7a is a five storey building located in Melbourne and has been designated an Importance Level 3 building as per the National Construction Code (NCC), Volume 1 (National Construction Code, 2019). The key characteristics of the building are as follows:

- The seismic design hazard (i.e. $k_p Z$) in accordance with AS 1170.4 is 0.10g.
- Seismic site classification of D_e (deep/soft soils).
- Ground-floor storey height of 5 m and upper-floor storey heights of 4.2 m.
- Floor masses of 0.77, 0.75, 0.75, 0.75 and 0.68 tonnes for the first through fifth stories, respectively.
- Lateral load resisting structural walls are 250 mm thick and 7 m long. The structural walls are constructed using N40 grade concrete and the vertical reinforcement consists of N20 bars at 200 mm centres on each face of the wall (reinforcement ratio of 0.013). The structural walls have an axial load of 4,900 kN for the seismic load case of $G + 0.3Q$.

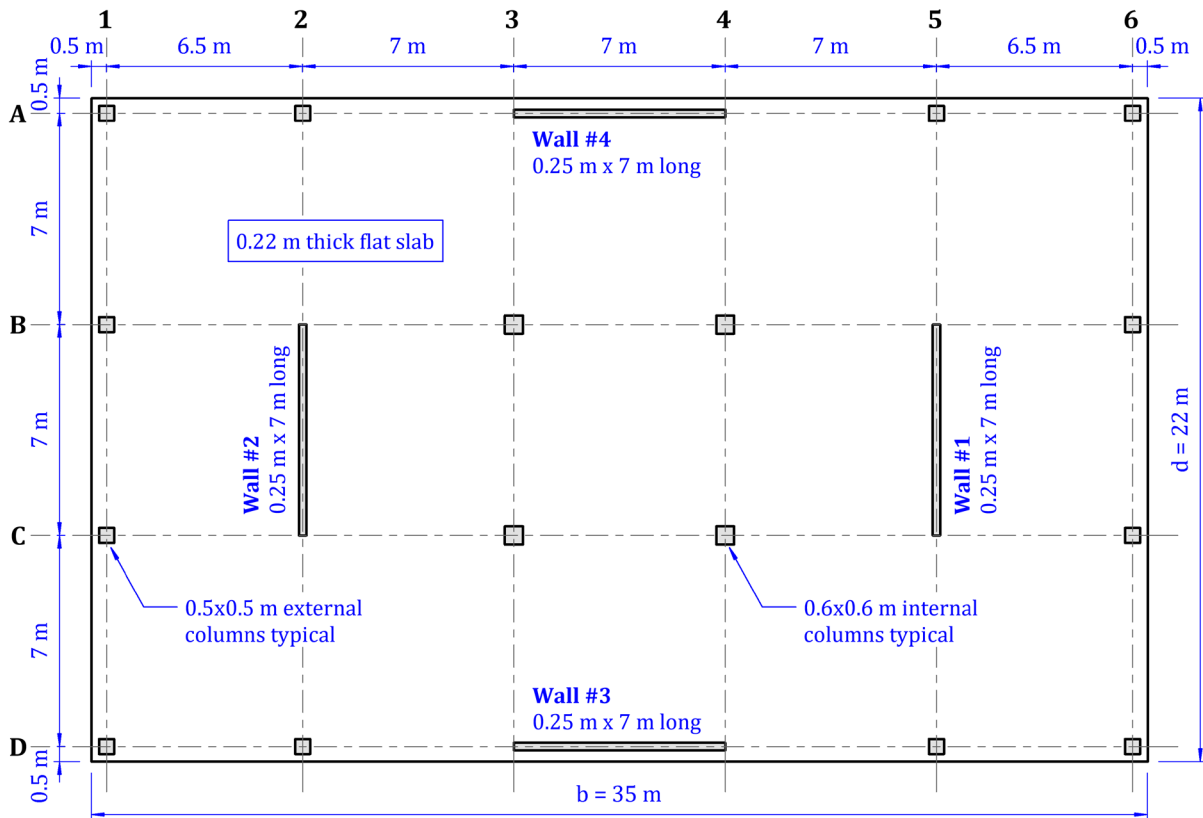


Figure 6: Case study building CSB7a (dimensions in mm unless otherwise specified).

7.2 Lateral force-displacement behaviour of structural walls

The non-linear lateral force-displacement behaviour of the structural walls can be calculated using an equivalent plastic hinge model, as illustrated in Figure 7, along with the stress-strain models, tension stiffening model and material properties presented in the previous sections.

The effective height (H_e) of the equivalent SDOF system that represents the five storey building is taken as 70% of the overall height (H) and similarly, the effective mass is taken as 70% of the total mass (m_{total}), which are both as per the recommendations in Priestley et al. (2007) for wall buildings. The seismic response of the equivalent SDOF element is assumed to have two components. This includes a linear yield curvature profile and as such, the yield displacement can be directly calculated by double integrating the linear curvature, resulting in $\Delta_y = \phi_y H_e^2 / 3$. Then, a plastic curvature (i.e. ϕ_p) is assumed to be constant over a length L_p at the base of the wall, which is referred to as the plastic hinge length. The plastic rotation (i.e. θ_p) is simply the plastic curvature multiplied by the plastic hinge length and therefore the plastic deformation (i.e. Δ_p) of the SDOF model is equal to the plastic rotation multiplied by the effective height, i.e. $\Delta_p = \phi_p L_p H_e$. The total displacement is then equal to the yield displacement plus the plastic displacement. The yield and plastic curvatures are determined from the non-linear moment curvature response of the wall's cross-section.

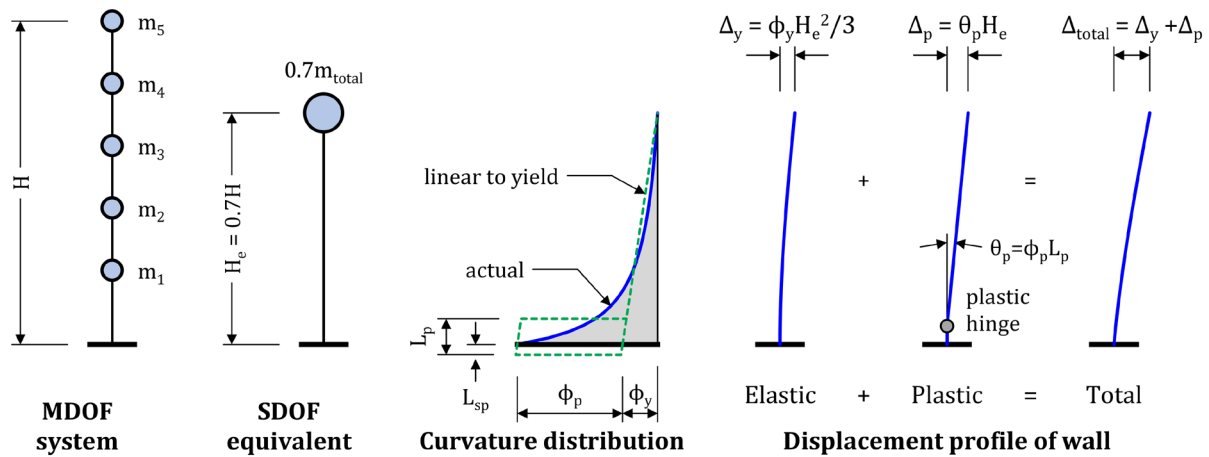


Figure 7: Plastic hinge model adopted for capacity spectrum method.

The authors have developed a simple and transparent non-linear fibre element analysis program for calculating the backbone moment-curvature and force-displacement response of rectangular and non-rectangular walls called WHAM (Menegon et al., 2020a). The program is a Microsoft Excel based application that can be downloaded free-of-charge from Menegon (2019). The program adopts the tension stiffening model and non-linear stress-strain material models proposed in this paper.

WHAM initially calculates the non-linear moment-curvature response of the cross-section and then determines the non-linear force-displacement response using the procedure shown in Figure 7. WHAM adopts the Priestley et al. (2007) model for plastic hinge length. The program has been validated against a database of experimental test results from 13 large-scale rectangular RC wall test specimens from five different test programs, which includes studies performed both locally and abroad. Very good correlation was observed between WHAM and the 13 rectangular walls (Menegon et al., 2020a), which included walls with shear-span ratios ranging from 2.0 to 6.5, axial load ratios from 3.5% to 12.8% and percentages of vertical reinforcement from 0.5% to 7.1%.

WHAM was used to determine the moment-curvature and force-displacement response of the structural walls in CSB7a (as shown in Figure 8) using the scenario 1 reinforcement properties in Table 1. The strain limits that triggered the performance limits in Table 2 are shown in brackets in the moment-curvature diagram (Figure 8(a)). The non-linear force-displacement behaviour in Figure 8(b) has been idealised into a 4-point response model to simplify the pushover analysis. The four points are: A, cracking; B, effective stiffness; C, yield; and D, ultimate. Point C (yield) is taken as the point corresponding to the yield capacity (i.e. the yield moment divided by the effective height, $F_y = M_y/H_e$) on a line projected from the origin through B (the effective stiffness point). Point D (ultimate) is taken as the ultimate displacement (based on the ultimate curvature) and the maximum load capacity of the wall (i.e. maximum moment capacity divided by effective height, $F_u = M_u/H_e$). The idealised model can be further simplified into a bilinear response model by ignoring the cracking point. The cracking point has been included in this example for completeness.

It should be noted that there is a further performance point (not shown here) associated with *actual* collapse, where the structure is no longer able to sustain the gravity loading. The displacement capacity of a structure at the collapse limit state is greater than the ultimate limit state and is dependent on both the axial load level and the level of confinement detailing. Further information is provided in Wilson et al. (2015) and Raza et al. (2019) about the maximum drift capacity of RC elements prior to axial load failure.

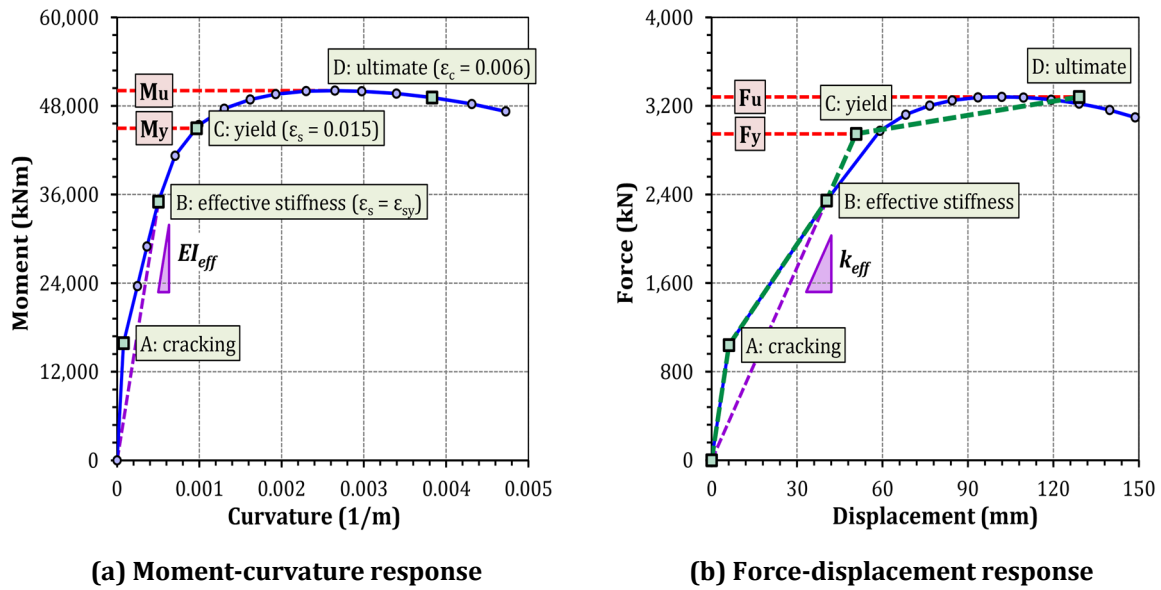


Figure 8: Lateral load capacity of the structural walls used in CSB7a.

7.3 Pushover analysis

The relatively simple floor plan with the same layout of structural walls from the ground level through to the roof level means that the pushover analysis could be performed by replacing each wall with a spring element that has the idealised 4-point non-linear force-displacement response in Figure 8(b). The four spring elements were connected to the centre of mass using rigid link elements, as illustrated in Figure 9. The centre of mass was offset by 10% of the width/depth of the building plan in each direction to account for accidental torsion, as per the requirements of AS 1170.4. Incrementally increasing displacements were then applied to the centre of mass.

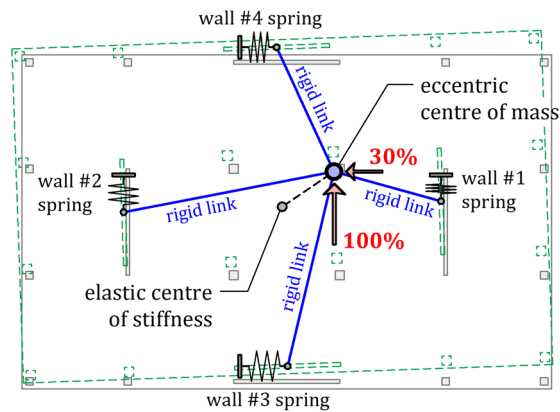


Figure 9: Idealised building model adopted in pushover analysis.

The analysis was initially performed by applying a unidirectional lateral displacement in the primary (100%) direction shown in Figure 9. The ensuring capacity curve overlaid on the ADRS diagram for CSB7a is presented in Figure 10(a). The vertical axis of the ADRS diagram is converted to force by multiplying RS_a by the effective mass of the structure, which in this case was taken as $m_{eff} = 0.7m_{total}$ (refer discussion above with reference to Figure 7). The analysis was then repeated as per the torsion requirements of AS 1170.4 by applying an additional (simultaneous) displacement in the secondary direction equal to 30% of the corresponding displacement being applied in the primary

direction (refer Figure 9 for the 100% and 30% directions). The ensuing capacity curve showing the building response is presented in Figure 10(b). It can be seen in these figures that although the displacement and pseudo lateral earthquake load of the performance point (i.e. Δ_d and F_d) is essentially the same in the primary (100%) direction, the ultimate displacement of the system is actually reduced from approximately 124 mm to 111 mm (~10%). This is due to the additional torsion induced from the orthogonal 30% displacement that results in wall #1 being subjected to higher individual displacement demands for the same corresponding overall system displacement. Irrespective, Figure 10(b) shows that the building performs adequately for the required seismic design hazard of $k_p Z = 0.10g$.

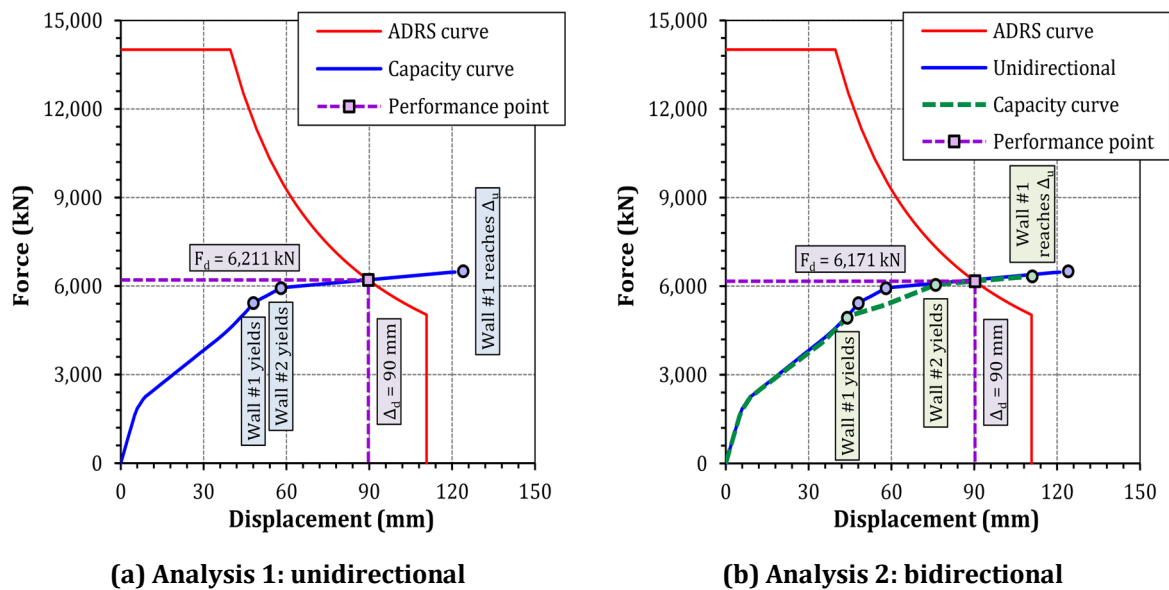


Figure 10: Seismic assessment of CSB7a using the capacity spectrum method.

7.4 Sensitivity analysis

AS 3600 requires a sensitivity analysis to be performed to assess how sensitive the results of the analysis are to variations in the input data and modelling parameters. Providing definitive advice on what should constitute a sensitivity analysis is outside the scope of this study. The extent of parameters that should be varied and the range over which they are modified to adequately fulfill the requirements of a sensitivity analysis will vary between structures. As such, it is difficult to provide firm guidance. With that said, an example of a sensitivity study is presented for CSB7a to illustrate how this activity could potentially be undertaken. This example is presented in lieu of any specific guidance in AS 3600 or its commentary. It may provide the starting point for developing the scope of a project specific sensitivity analysis.

In this example, six different sets of input parameters were systematically varied and the effects this had on the system level response of the building were observed. The authors have selected the parameters to be varied and the range over which they are varied based on their experience and knowledge gained through multiple large-scale experimental testing programs of RC walls and columns (e.g. Wibowo et al. (2014); Menegon et al. (2017a); Menegon et al. (2019a); Menegon et al. (2020b); Menegon et al. (2020c); Raza et al. (2020a); Raza et al. (2020b); Raza et al. (2020c)).

A summary of the input parameters that were varied is presented in Table 3 and comparisons of the system level building response are provided in Figure 11. The baseline response in these comparisons is the result shown in Figure 10(b).

The first three sets of input parameters that were considered relate to the reinforcement properties. Initially the model was re-run with the two different sets of supplier scenario reinforcement properties presented in Table 1. Following this, a variation in the yield stress of ± 1.5 times the standard deviation (i.e. ± 34.7 MPa) was considered, followed by, a variation in the ultimate strain of ± 1.5 times the standard deviation (i.e. $\pm 2.8\%$). A typical approach for accounting for variation is to consider the mean value plus/minus one standard deviation, which should theoretically account for approximately two-thirds of the population. However, to examine the more extreme conditions, the authors have adopted a material value range of ± 1.5 times the standard deviation. The standard deviations were taken from the material test database referenced earlier (i.e. Menegon et al., 2021a). These three comparisons are presented in Figures 11(a), 11(b) and 11(c), respectively.

Next, the compressive strength of the concrete was varied by ± 1.5 times the standard deviation (i.e. ± 5.3 MPa). The standard deviation was taken as 0.125 times the concrete strength as per Menegon et al. (2021a). The axial load was then varied by $\pm 30\%$, and finally, the plastic hinge length adopted in the analysis was varied by $\pm 20\%$. These three comparisons are presented in Figures 11(d), 11(e) and 11(f), respectively.

It can be seen in each of these figures that the respective variation in input parameters did not change the response significantly. In each scenario, the ultimate displacement and ultimate lateral capacity did not vary by more than (plus/minus) 5–15%.

Table 3: Summary of input parameters adopted in sensitivity analysis.

	Variation 1	Variation 2	Variation 3
Description	Reinforcement property scenarios (Table 1)	Yield stress ± 1.5 standard deviations	Ultimate strain ± 1.5 standard deviations
Baseline	$f_{sy} = 550$ MPa $f_{su}/f_{sy} = 1.22$ $\varepsilon_{su} = 10.3\%$	$f_{sy} = 550$ MPa $f_{su}/f_{sy} = 1.22$ $\varepsilon_{su} = 10.3\%$	$f_{sy} = 550$ MPa $f_{su}/f_{sy} = 1.22$ $\varepsilon_{su} = 10.3\%$
Scenario 1	$f_{sy} = 530$ MPa $f_{su}/f_{sy} = 1.29$ $\varepsilon_{su} = 12.0$	$f_{sy} = 498$ MPa $f_{su}/f_{sy} = 1.22$ $\varepsilon_{su} = 10.3\%$	$f_{sy} = 550$ MPa $f_{su}/f_{sy} = 1.22$ $\varepsilon_{su} = 6.1\%$
Scenario 2	$f_{sy} = 560$ MPa $f_{su}/f_{sy} = 1.13$ $\varepsilon_{su} = 6.0\%$	$f_{sy} = 602$ MPa $f_{su}/f_{sy} = 1.22$ $\varepsilon_{su} = 10.3\%$	$f_{sy} = 550$ MPa $f_{su}/f_{sy} = 1.22$ $\varepsilon_{su} = 14.5\%$
	Variation 4	Variation 5	Variation 6
Description	Concrete strength ± 1.5 standard deviations	Axial load variation by $\pm 30\%$	Plastic hinge length variation by $\pm 20\%$
Baseline	$f_{cmi} = 42.4$ MPa	$N^* = 4,900$ kN	$L_p = 1.60$ m
Scenario 1	$f_{cmi} = 34.5$ MPa	$N^* = 3,430$ kN	$L_p = 1.28$ m
Scenario 2	$f_{cmi} = 50.4$ MPa	$N^* = 6,370$ kN	$L_p = 1.92$ m

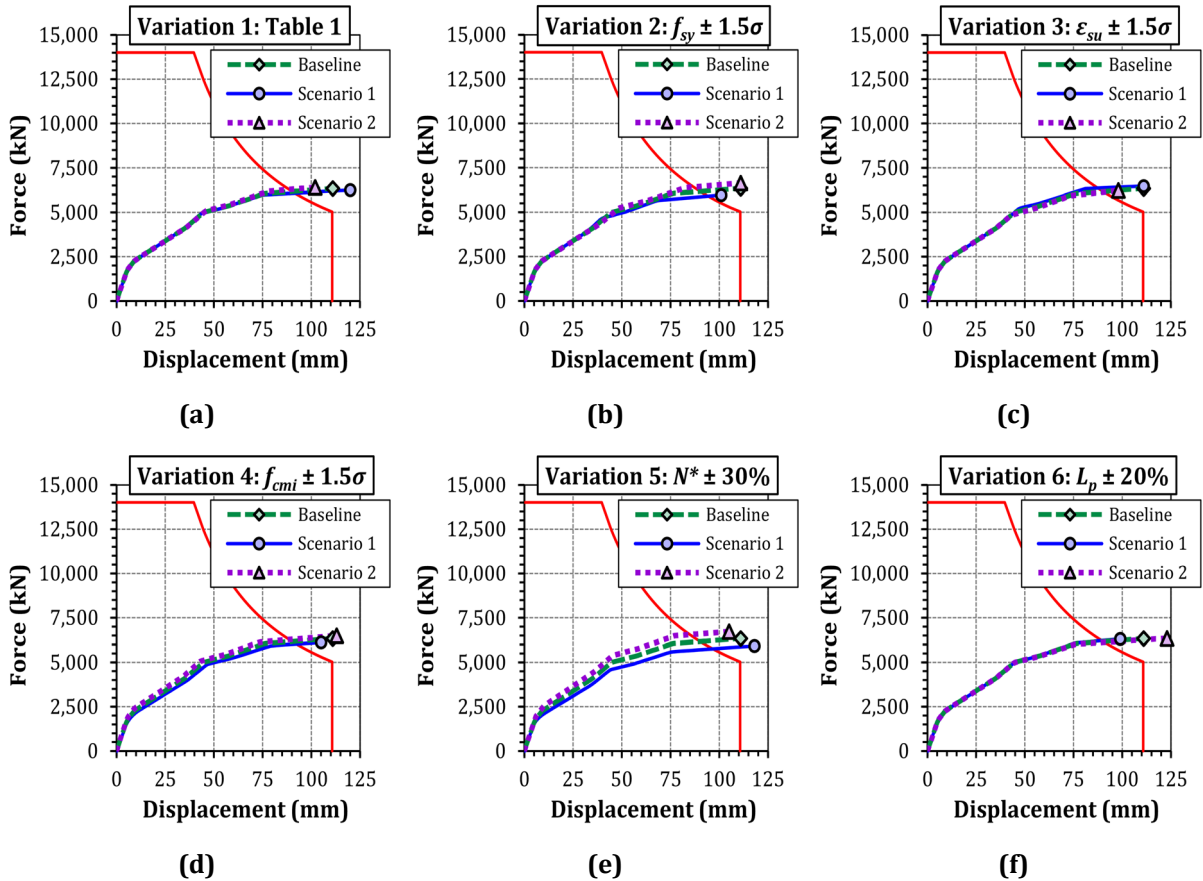


Figure 11: Sensitivity analysis results.

It should be noted that while the variation in reinforcement properties seemingly led to little variation in the overall ultimate response in this instance; this may not always be the case. Rectangular walls are usually compression-controlled elements, in that the ultimate performance is usually controlled by the concrete compressive strain limits in Table 2. Whereas, non-rectangular walls (i.e. box-shaped core walls around lift shafts) can often be tension-controlled elements where the ultimate performance is controlled by tension strain limits in the vertical reinforcement. Under this latter scenario, a variation in reinforcement properties can have a much more significant effect on the ultimate performance. Non-rectangular walls like building cores are usually tension-controlled because they have large compressive flanges, which means the neutral axis depth of the section can be much shallower and result in significantly higher tension strains for a corresponding level of curvature than in a rectangular wall with a deeper neutral axis depth.

7.5 Other considerations and design checks

Other issues that need to be assessed by the designer when adopting this displacement-based assessment procedure, which are outside the scope of this paper, include:

1. The walls need to be adequately detailed to ensure that shear failure cannot occur since the non-linear performance relies on the development of a flexure-based plastic hinge at the base of the wall. This could simply be achieved by ensuring the design shear capacity of the wall was an appropriate amount higher (e.g. 20%) than the corresponding maximum lateral capacity based on the flexural response (i.e. F_u in Figure 8(b)).

2. Ensure the gravity columns can sustain the amount of lateral drift corresponding to the performance point of the structure. The unidirectional Raza et al. (2018) or bidirectional Raza et al. (2020c) column drift models could be adopted in this instance.

8 Summary and conclusions

Displacement-based (DB) seismic design procedures offer many benefits over traditional force-based (FB) seismic design procedures. DB procedures allow designers to directly and more accurately calculate the non-linear behaviour (capacity) of the building, which is in direct contrast to FB procedures where the non-linear capacity is broadly assigned based on the basic structural form and level of detailing stipulated by the code. The latter is a key shortcoming of FB design.

A detailed framework is outlined in this paper for undertaking a DB seismic assessment in accordance with the requirements of the Australian Standard for earthquake actions, AS 1170.4 and the Australian Standard for concrete structures, AS 3600. Recommendations and appropriate commentary are provided for the various requirements stipulated by both standards for adopting a design/assessment method of this nature. The recommendations are provided in the context of a typical RC wall building and include a tension stiffening model, non-linear stress-strain material models, mean material properties for concrete and reinforcement and material strain limits.

The paper is concluded with a case study example to show how a DB procedure can be used to assess the seismic performance of a typical multi-storey building. The non-linear displacement behaviour of the lateral load resisting elements are calculated using a fibre-element analysis procedure (using the software WHAM) that adopts the various recommendations in the paper.

The case study example also features a 'sensitivity analysis' to assess how the individual inputs of the non-linear modelling procedure affects the overall system level response. The sensitivity analysis considered variations in material properties (both reinforcement and concrete), axial load and plastic hinge length. Despite significant variations being considered, the ultimate response was within 5–15% of the baseline response.

Acknowledgements

The authors acknowledge the financial supports from the Australian Research Council (ARC) Discovery Project DP180101593 entitled *Seismic Performance of Precast Concrete Buildings for Lower Seismic Regions*.

Notes on contributors

Scott Menegon is a Research Fellow at Swinburne University of Technology and a Senior Structural Engineer at the national consulting engineering firm Wallbridge Gilbert Aztec (WGA). Scott is also a Group Technical Lead at WGA with a focus on innovation and technical development. He received his BEng (Hons) from Queensland University of Technology; MEngStruct from the University of Melbourne; and PhD from Swinburne University of Technology. His primary research interests include reinforced concrete; precast concrete; earthquake engineering; and collision actions. Scott is a member of the seismic sub-committee for AS 3600 and his research contributions to seismic design in Australia were recently recognised through being awarded the 2019 RW Chapman Medal from Engineers Australia.

Hing-Ho Tsang is an Associate Professor at Swinburne University of Technology, Melbourne, Australia. He received his BEng (Hons) and PhD from the University of Hong Kong. His research and engagement works have contributed to the 2018 Amendment of AS 1170.4, as well as the development of seismic design codes

respectively for Hong Kong, China and Malaysia. Hing-Ho's research interests include structural design and protective technology for extreme events.

John Wilson is a Professor, Deputy Vice-Chancellor and Chief Executive Officer of Swinburne Sarawak, Malaysia. He received his BEng (Hons) from Monash University; MSc from the University of California, Berkeley; and PhD from the University of Melbourne. John is the chairman of BD6/11, the committee responsible for AS 1170.4. John's research interests are focused on earthquake engineering with a particular emphasis on the seismic performance of limited ductile RC columns and walls.

Nelson Lam is a Professor of Civil Engineering at the University of Melbourne, Australia. He received his BSc from the University of Leeds; MSc from Imperial College of Science & Technology; and PhD from the University of Melbourne. Nelson is a member of BD6/11, the committee responsible for AS 1170.4, and an international advisor to the drafting of the Malaysian National Annex to Eurocode 8. Nelson's research interests include the behaviour of RC buildings in lower seismic regions, ground motion analysis, structural dynamics and impact dynamics.

References

Applied Technology Council, 1996, *ATC 40 Seismic evaluation and retrofit of concrete buildings*, Applied Technology Council, Redwood City, CA.

Chai, Y.H. and Elayer, D.T., 1999, "Lateral Stability of Reinforced Concrete Columns under Axial Reversed Cyclic Tension and Compression", *ACI Structural Journal*, Vol. 96(5), pp. 780-789.

Collins, M.P., Mitchell, D. and MacGregor, J.G., 1993, "Structural Design Considerations for High-Strength Concrete", *Concrete International: Design and Construction*, Vol. 15(5).

Dashti, F., Dhakal, R.P. and Pampanin, S., 2017, "Tests on slender ductile structural walls designed according to New Zealand Standard", *Bulletin of the New Zealand Society for Earthquake Engineering*, Vol. 50(4), pp. 504-516.

Elwood, K.J., 2013, "Performance of concrete buildings in the 22 February 2011 Christchurch earthquake and implications for Canadian codes", *Canadian Journal of Civil Engineering*, Vol. 40(3), pp. 759-776.

Federal Emergency Management Agency, 1997a, *FEMA 273 NEHRP Guidelines for the Seismic Rehabilitation of Buildings*, Federal Emergency Management Agency, Washington, DC.

Federal Emergency Management Agency, 1997b, *FEMA 274 NEHRP Commentary on the Guidelines for the Seismic Rehabilitation of Buildings*, Federal Emergency Management Agency, Washington, DC.

Karthik, M.M. and Mander, J.B., 2011, "Stress-Block Parameters for Unconfined and Confined Concrete Based on a Unified Stress-Strain Model", *Journal of Structural Engineering*, Vol. 137(2), pp. 270-273.

Kent, D.C. and Park, R., 1971, "Flexural Members with Confined Concrete", *ASCE Journal of the Structural Division*, Vol. 97(7), pp. 1969-1990.

Li, B., Park, R. and Tanaka, T., 2000, "Constitutive Behaviour of High-Strength Concrete Under Dynamic Loads", *ACI Structural Journal*, Vol. 97(4), pp. 619-629.

Looi, D.T.W., Tsang, H.H. and Lam, N.T.K., 2019, "The Malaysian seismic design code: lessons learnt", *Proceedings of the 2019 Pacific Conference on Earthquake Engineering, 4-6 April*, Auckland, New Zealand.

Mander, J.B., Priestley, M.J.N. and Park, R., 1988, "Theoretical stress-strain model for confined concrete", *ASCE Journal of Structural Engineering*, Vol. 114(8), pp. 1827-1849.

Menegon, S.J., Wilson, J.L., Lam, N.T.K. and Gad, E.F., 2017a, "Experimental testing of reinforced concrete walls in regions of lower seismicity", *Bulletin of the New Zealand Society for Earthquake Engineering*, Vol. 50(4), pp. 494-503, doi:10.5459/bnzsee.50.4.494-503.

Menegon, S.J., Wilson, J.L., Lam, N.T.K. and Gad, E.F., 2017b, "RC Walls in Australia: Reconnaissance Survey of Industry and Literature Review of Experimental Testing", *Australian Journal of Structural Engineering*, Vol. 18(1), pp. 24-40, doi:10.1080/13287982.2017.1315207.

- Menegon, S.J., Wilson, J.L., Lam, N.T.K. and McBean, P., 2018, "RC Walls in Australia: Seismic Design and Detailing to AS 1170.4 and AS 3600", *Australian Journal of Structural Engineering*, Vol. 19(1), pp. 67-84, doi:10.1080/13287982.2017.1410309.
- Menegon, S.J., Wilson, J.L., Lam, N.T.K. and Gad, E.F., 2019a, "Experimental testing of nonductile RC wall boundary elements", *ACI Structural Journal*, Vol. 116(6), pp. 213-225, doi:10.14359/51718008.
- Menegon, S.J., Tsang, H.H., Lumantarna, E., Lam, N.T.K., Wilson, J.L. and Gad, E.F., 2019b, "Framework for seismic vulnerability assessment of reinforced concrete buildings in Australia", *Australian Journal of Structural Engineering*, Vol. 20(2), pp. 143-158, doi:10.1080/13287982.2019.1611034.
- Menegon, S.J. (2019), *WHAM: a user-friendly and transparent non-linear analysis program for RC walls and building cores*, available from: downloads.menegon.com.au/1/20190901.
- Menegon, S.J., Wilson, J.L., Lam, N.T.K. and Gad, E.F., 2020a, "Development of a user-friendly and transparent non-linear analysis program for RC walls", *Computers and Concrete*, Vol. 25(4), pp. 327-341, doi:10.12989/cac.2020.25.4.327.
- Menegon, S.J., Wilson, J.L., Lam, N.T.K. and Gad, E.F., 2020b, "Experimental assessment of the ultimate performance and lateral drift behaviour of precast concrete building cores", *Advances in Structural Engineering*, Vol. 23(12), pp. 2597-2613, doi:10.1177/1369433220919077.
- Menegon, S.J., Wilson, J.L., Lam, N.T.K. and Gad, E.F., 2020c, "Experimental Testing of Innovative Panel-to-Panel Connections for Precast Concrete Building Cores", *Engineering Structures*, Vol. 207, Article number 110239, doi:10.1016/j.engstruct.2020.110239.
- Menegon, S.J., Tsang, H.H., Wilson, J.L. and Lam, N.T.K., 2021a, "Statistical analysis of material properties and recommended values for the assessment of RC structures in Australia", *Australian Journal of Structural Engineering*, doi:10.1080/13287982.2021.1946993.
- Menegon, S.J., Wilson, J.L., Lam, N.T.K. and Gad, E.F., 2021b, "Tension stiffening model for limited ductile reinforced concrete walls", *Magazine of Concrete Research*, Vol. 73(7), pp. 366-378.
- Moehle, J.P., 1992, "Displacement-Based Design of RC Structures Subjected to Earthquakes", *Earthquake Spectra*, Vol. 8(3), pp. 403-428.
- National Construction Code, 2019, *National Construction Code 2019, Volume One, Building Code of Australia, Class 2 to Class 9 Buildings*, The Australian Building Codes Board, Canberra, ACT.
- Neville, A.M., 1996, *Properties of Concrete*, 4th ed., Longman Group UK, Harlow, Essex.
- Park, R., Priestley, M.J.N. and Gill, W.D., 1982, "Ductility of Square-Confined Concrete Columns", *ASCE Journal of the Structural Division*, Vol. 108(4), pp. 929-950.
- Pitilakis, K., Riga, E., Anastasiadis, A., Fotopoulou, S. and Karafagka, S., 2019, "Towards the revision of EC8: Proposal for an alternative site classification scheme and associated intensity dependent spectral amplification factors", *Soil Dynamics and Earthquake Engineering*, Vol. 126, Article number 105137, doi:10.1016/j.soildyn.2018.03.030.
- Priestley, M.J.N. and Park, R., 1987, "Strength and Ductility of Concrete Bridge Columns Under Seismic Loading", *ACI Structural Journal*, Vol. 84(1), pp. 61-76.
- Priestley, M.J.N., Seible, F. and Calvi, G.M., 1996, *Seismic Design and Retrofit of Bridges*, Wiley, New York.
- Priestley, M.J.N. and Kowalsky, M.J., 2000, "Direct Displacement-Based Seismic Design of Concrete Buildings", *Bulletin of the New Zealand Society for Earthquake Engineering*, Vol. 33(4), pp. 421-444.
- Priestley, M.J.N., Calvi, G.M. and Kowalsky, M.J., 2007, *Displacement-Based Seismic Design of Structures*, IUSS Press, Pavia, Italy.
- Priestley, N.J.M., 1993, "Myths and Fallacies in Earthquake Engineering - Conflicts Between Design and Reality", *Bulletin of the New Zealand Society for Earthquake Engineering*, Vol. 26(3), pp. 329-341.
- Raza, S., Tsang, H.H. and Wilson, J.L., 2018, "Unified models for post-peak failure drifts of normal and high strength RC columns", *Magazine of Concrete Research*, Vol. 70(21), pp. 1081-1101.
- Raza, S., Tsang, H.H., Menegon, S.J. and Wilson, J.L., 2019, *Seismic Performance Assessment of Reinforced Concrete Columns in Regions of Low to Moderate Seismicity*, in *Resilient Structures and Infrastructure*, Springer, Singapore, pp. 269-286.

- Raza, S., Menegon, S.J., Tsang, H.H. and Wilson, J.L., 2020a, "Axial Load Variation of Columns in Symmetrical RC Buildings Subject to Bidirectional Lateral Actions in Regions of Low to Moderate Seismicity", *Journal of Earthquake Engineering*, doi:10.1080/13632469.2020.1772151.
- Raza, S., Menegon, S.J., Tsang, H.H. and Wilson, J.L., 2020b, "Collapse Performance of Limited Ductile High-Strength RC Columns Under Uni-Directional Cyclic Actions", *Journal of Structural Engineering*, Vol. 146(10), Article number 4020201, doi:10.1061/(ASCE)ST.1943-541X.0002772.
- Raza, S., Menegon, S.J., Tsang, H.H. and Wilson, J.L., 2020c, "Force-Displacement Behavior of Limited Ductile High-Strength RC Columns under Bidirectional Earthquake Actions", *Engineering Structures*, Vol. 208, Article number 110278, doi:10.1016/j.engstruct.2020.110278.
- Scott, B.D., Park, R. and Priestley, M.J.N., 1982, "Stress-strain Behavior of Concrete Confined by Overlapping Hoops at Low and High Strain Rates", *ACI Structural Journal*, Vol. 79(1), pp. 13-27.
- Shibata, A. and Sozen, M., 1976, "Substitute Structure Method for Seismic Design in R/C", *Journal of the Structural Division*, Vol. 102(1), pp. 1-18.
- Shimazaki, K. and Sozen, M.A., 1984, *Seismic Drift of Reinforced Concrete Structures*, Technical Research Report of Hazama-Gumi Ltd., Tokyo, Japan.
- Standards Australia, 2007, *AS 1170.4-2007 Structural design actions, Part 4: Earthquake actions in Australia*, Standards Australia, Sydney, NSW.
- Standards Australia, 2014, *AS 3600 Supplement 1:2014 Concrete Structures-Commentary*, SAI Global Limited, Sydney, NSW.
- Standards Australia, 2018, *AS 3600:2018 Concrete structures*, Standards Australia Limited, Sydney, NSW.
- Standards Australia and Standards New Zealand, 2002, *AS/NZS 1170.0:2002 Structural design actions, Part 0: General principles*, SAI Global Limited and Standards New Zealand, Sydney and Wellington.
- Standards Australia and Standards New Zealand, 2019, *AS/NZS 4671:2019 Steel for the reinforcement of concrete*, Standards Australia Limited and Standards New Zealand, Sydney and Wellington.
- Sullivan, T.J., Priestley, M.J.N. and Calvi, G.M. (Editors), 2012, *A Model Code for the Displacement-Based Seismic Design of Structures*, IUSS Press, Pavia, Italy.
- Tsang, H.H., Chandler, A.M. and Lam, N.T.K., 2006, "Estimating non-linear site response by single period approximation", *Earthquake Engineering and Structural Dynamics*, Vol. 35(9), pp. 1053-1076.
- Tsang, H.H., Wilson, J.L., Lam, N.T.K. and Su, R.K.L., 2017a, "A design spectrum model for flexible soil sites in regions of low-to-moderate seismicity", *Soil Dynamics and Earthquake Engineering*, Vol. 92, pp. 36-45.
- Tsang, H.H., Wilson, J.L. and Lam, N.T.K., 2017b, "A refined design spectrum model for regions of lower seismicity", *Australian Journal of Structural Engineering*, Vol. 18(1), pp. 3-10.
- Wallace, J.W. and Moehle, J.P., 1992, "Ductility and Detailing Requirements of Bearing Wall Buildings", *Journal of Structural Engineering*, Vol. 118(6), pp. 1625-1644.
- Wallace, J.W., 1994, "New Methodology for Seismic Design of RC Shear Walls", *Journal of Structural Engineering*, Vol. 120(3), pp. 863-884.
- Wibowo, A., Wilson, J., Lam, N. and Gad, E., 2014, "Drift capacity of lightly reinforced concrete columns", *Australian Journal of Structural Engineering*, Vol. 15(2), pp. 131-150.
- Wilson, J. and Lam, N., 2006, "Earthquake design of buildings in Australia using velocity and displacement principles", *Australian Journal of Structural Engineering*, Vol. 6(2), pp. 103-118.
- Wilson, J. and Lam, N. (Editors), 2007, *AS 1170.4 Supp1-2007 Commentary to Structural Design Actions Part 4: Earthquake Actions in Australia*, Australian Earthquake Engineering Society, McKinnon, VIC.
- Wilson, J.L., Wibowo, A., Lam, N.T.K. and Gad, E.F., 2015, "Drift Behaviour of Lightly Reinforced Concrete Columns and Structural Walls for Seismic Performance Assessment", *Australian Journal of Structural Engineering*, Vol. 16(1), pp. 62-74.